Structure and Dynamics of Hydronium in the Ion Channel Gramicidin A

Diane E. Sagnella and Gregory A. Voth
Department of Chemistry, University of Pennsylvania, Philadelphia, Pennsylvania 19104-6323 USA

ABSTRACT The effects of the hydronium ion, H_3O^+, on the structure of the ion channel gramicidin A and the hydrogen-bonded network of waters within the channel were studied to help elucidate a possible mechanism for proton transport through the channel. Several classical molecular dynamics studies were carried out with the hydronium in either the center of a gramicidin monomer or in the dimer junction. Structural reorganization of the channel backbone was observed for different hydronium positions, which were most apparent when the hydronium was within the monomer. In both cases the average O-O distance between the hydronium ion and its nearest neighbor water molecule was found to be ~2.55 Å, indicating a rather strong hydrogen bond. Importantly, a subsequent break in the hydrogen-bonded network between the nearest neighbor and the next-nearest neighbor (~2.7–3.0 Å) was repeatedly observed. Moreover, the carbonyl groups of gramicidin A were found to interact with the charge on the hydronium ion, helping in its stabilization. These facts may have significant implications for the proton hopping mechanism. The presence of the hydronium ion in the channel also inhibits to some degree the reorientational motions of the channel water molecules.

INTRODUCTION

The migration, or "translocation," of protons in biological systems is a process of fundamental importance. The flow of protons, for example, is coupled to the flow of electrons in such processes as ATP synthesis through the chemiosmotic mechanism. There has been considerable speculation as to the role of water molecules in the proton diffusion mechanism. For example, in bulk water it is well known that the mobility of hydronium is ~5 times greater than that of an ion of similar ionic radius (i.e., K^+). This suggests that a different mechanism is operational in the diffusion of protons than that for other ions. To date the most commonly accepted mechanism believed to describe this anomaly is that of Grotthus. In the Grotthus "shuttle" picture, the hydrogen-bonded network of water molecules offers a dynamical bridge for proton hopping. Other ions cannot take advantage of this bridge, so they must diffuse normally via hydrodynamic diffusion. The result of the Grotthus mechanism is not the diffusion of an individual proton, but rather a translocation of the charge.

In a variety of biosystems, protons are thought to be transported with the help of intervening water molecules. For example, it has even been observed that membranes exhibit an enhanced permeability to protons that exceeds that of other monovalent ions (Nichols and Deamer, 1978; Nichols and Deamer, 1980; Nichols et al., 1980; Deamer and Nichols, 1983). To explain this it has been proposed that hydrogen-bonded chains of water, water wires, can exist within such hydrophobic environments, along which protons can shuttle. To date there is evidence to support this theory (Nagle and Tristram-Nagle, 1983). Actual evidence for the existence of such pathways has been seen in systems such as the photosynthetic reaction center (Deisenhofer and Michel, 1989) and the CF_0 channel of bacteriorhodopsin (Henderson et al., 1990; Cao et al., 1991; Papadopoulos et al., 1990). Both systems are intricately involved in energy transduction and the oxidation cycle of cellular respiration.

To explore the mechanism behind proton transfer within complex biological systems a suitable model must be used. A common system in the theoretical study of ion translocation is the ion channel gramicidin A (gA). Furthermore, gA has been used as a prototype in experiments designed to explain and justify the existence of the water wire's role in proton diffusion in biological systems (Deamer, 1987). Gramicidin A is a membrane spanning channel that is highly monovalent selective. It has been studied extensively, both experimentally (Hladky and Haydon, 1972; Myers and Haydon, 1972) and theoretically (for a review, see Roux and Karplus, 1994) as an ion channel and is well characterized. Whereas gA greatly facilitates the transport of ions such as Na^+ and K^+, it also allows for anomalously high rates of proton translocation relative to these other ions (Akeson and Deamer, 1991). This behavior has been attributed to the linear array of water molecules within the channel. The work of Levitt et. al. (1978), in which the streaming potential that accompanies Na^+ or K^+ diffusion was decidedly absent in the case of proton diffusion, supports this idea. The narrow size of gA would require monovalent cations other than H_3O^+ to push the enclosed water molecules through the channel, creating the streaming potential; but in the case of H_3O^+ diffusion occurs via the channel waters. Therefore, it is likely that the mechanism

Received for publication 7 November 1995 and in final form 1 February 1996.

Address reprint requests to Dr. Gregory A. Voth, Department of Chemistry, University of Pennsylvania, 231 S. 34th Street, Philadelphia, PA 19104-6323. Tel.: 215-898-3048; Fax: 215-573-2112; E-mail: voth@a.chem.upenn.edu.

0006-3495/96/05/2043/09 $2.00

of proton diffusion through gA is similar to that believed to occur in many other complex systems, including liquid water and ice. This fact, along with its structural simplicity and relatively small size, makes gA an ideal system for the study of proton translocation along hydrogen-bonded chains of waters in biosystems.

Structurally, gA is a dimer formed by the head-to-head contact of two 15-residue polypeptides of alternating L and D amino acids of sequence: HCO-L-Val^{1}-Gly^{2}-L-Ala^{3}-D-Leu^{4}-L-Ala^{5}-D-Val^{6}-L-Val^{7}-D-Val^{8}-L-Trp^{9}-D-Leu^{10}-L-Trp^{11}-D-Leu^{12}-L-Trp^{13}-D-Leu^{14}-L-Trp^{15}-NHCH$_2$CH$_2$OH (Sarges and Witkop, 1965). The ion channel is a β helix (Urry, 1971) whose handedness has been a subject of debate over the past few years. Recent work, however, indicates a right-handed helix (Arseniev et al., 1985; Nicholson and Cross, 1989). The hydrophobic side chains of the channel point outward from the channel axis, whereas the carbonyl groups line the lumen. The position of the carbonyls effectively solvates the enclosed waters and ions, lowering the barrier to ion diffusion across the nonpolar membrane environment.

To better elucidate the possible mechanism of proton transfer within gA, the results of several molecular dynamics (MD) simulations that focus on the effects of a hydronium ion on the structure of the gA and on the chain of waters within it are reported in the present paper. The barrier-to-proton transfer in the $H_5O_2^+$ complex in bulk water is determined by the O-O distance, which increases as the donor and acceptor move apart. However, there is significant theoretical evidence that the rate determining step to proton transfer is the dynamics of the second solvation shell. The next-nearest neighbor (NNN) waters must come in and form strong hydrogen bonds with the nearest neighbors (NN) for the proton to be passed (Tuckerman et al., 1995; Lobaugh and Voth, 1996). It is this type of behavior that appears to be necessary for the Grotthus mechanism to be at work in water. In gA, we have found that the hydronium ion tends to draw its NN waters in to an average O-O distance of 2.55 Å. This is considerably shorter than the average channel water O-O distance (2.78 Å) and consistent with that found for the $H_5O_2^+$ complex in water. Strangely enough, the next hydrogen bond in the channel is actually longer than the average channel water-water O-O distance. However, also in the second solvation shell are carbonyl oxygens, which can act to effectively stabilize the hydronium ion. Often times a carbonyl oxygen is in closer proximity to the first solvation shell than the next channel water. These results illustrate the importance of the molecular details within the channel as opposed to a purely dielectric continuum picture.

METHODS

The biomolecular model used in the present studies is similar to that of Roux and Karplus (RK) (1993). This model packs Lennard-Jones (LJ) spheres, the size of a methyl group, around the channel to provide a hydrophobic environment for the side chains and to lend support to the channel. Bulk water molecules are then placed at the ends of the channel. Whereas the RK model employed a Langevin region as a boundary for the membrane and bulk water, our system is periodic in the x, y, and z directions for the bulk water and in the xy plane for the LJ spheres. Like RK, we harmonically constrain the LJ spheres in the z direction to prevent diffusion of the membrane into the bulk water.

The gA system was constructed as follows. First, eight channel water oxygen nuclei were placed inside the channel, leaving space for the hydronium ion. Hydrogen nuclei were then added, oriented randomly about their parent oxygen; this procedure was designed to prevent accidental placement of the waters in a local minimum. Then, the LJ spheres were added. A grid of these spheres was overlaid and those within 2.165 Å of a previously placed atom were removed. This membrane spans 24 Å along the length of the channel and is 12 Å from the channel axis. Next, to ensure solvation of the channel mouths, a cap of water oxygen nuclei was placed at each end of the channel in the same fashion as the LJ spheres and the hydrogens were added and then randomly oriented. Finally, bulk water molecules were added. The latter was done by splitting in two a previously equilibrated box of waters and separating these pieces by the length of the channel. The dimensions of the entire system were 24×24×41 Å^3 in the x, y, and z directions, respectively.

The all atom structure used in the simulations was obtained from R. E. Koeppe (*personal communication*). The parameters for the protein and protein-water interactions were those of the CHARMM parameter set (param22). The TIP3P water model was used for the bulk and channel waters (Jorgensen et al., 1983). However, the MD software used for the dynamics and calculations was developed in our laboratory. A time step of 0.5 fs was used to integrate the equations of motion. Equilibration of the system was carried out at 300 K. This process involved a complete velocity redistribution every 2 ps, or when the temperature as defined by the kinetic energy went outside of some specified tolerance (5%). The resampling of velocities was combined with the Andersen thermostatting method (Anderson, 1980) of velocity change for random atoms in the system. Every 10 time steps an atom was randomly selected from the channel, the membrane, and the bulk waters and was reassigned a velocity selected from the Boltzmann distribution. For the channel waters an oxygen and a proton were randomly chosen. This thermostatting was carried out for ~50 ps.

In an attempt to gauge the degree of nonergodicity in the MD simulations, two different initial conditions with respect to the O-O distances of the channel waters were used. The first (b1) left a 3.0-Å buffer from the mouth of the channel (defined as being 12 Å from the center) in which channel waters were not originally placed. This procedure resulted in a channel water O-O distance of 2.25 Å. The second initial condition (b2) corresponded to a 1.5-Å buffer from the channel mouth and resulted in an O-O distance of 2.63 Å. The entire system was composed of 1603 atoms for b1 (552 channel atoms, 8 channel waters, 1 hydronium ion, 234 LJ spheres, and 263 Bulk waters (14 cap, 249 others)) and 1585 atoms in b2 (only 8 cap waters). The change in bulk water density between the two systems was ~2%. The use of the two different starting conditions proved to be informative when the hydronium was in the dimer junction

For the first 20 ps of the simulations the cap waters were harmonically restrained to stay within the vicinity of the channel mouth. The harmonic constraint was put into effect when the water drifted away from the radius of the cap (r_{cap} = 4 Å). The restraining potential was taken to be of the form

$$V_{cap} = \frac{k_{cap}}{2}(r_i - r_{cap})^2 \quad (1)$$

where i represents the particular water molecule and r_i is defined as

$$r_i = (x_i^2 + y_i^2 + (|z_i| - z_{cap})^2)^{1/2} \quad (2)$$

The parameters z_{cap} and k_{cap} were 10 Å and 0.5 kcal/mol Å^{-2}, respectively. For the b2 initial conditions, it was observed that the end waters tended to diffuse away from the channel, but cap waters would then take their place. No restraints were kept on the waters when the statistical or dynamical averaging, reported in the following sections, was carried out.

The gA channel itself was constrained so that the center of mass of the dimer remained at the position (0,0,0) and the center of mass of the monomers remained at (0,0,−z) and (0,0,z). Using the method of Lagrange multipliers, it can be shown that this constraint amounts to subtracting out the respective center of mass coordinate (CM) from the original. The system moves without constraint, then after each move the dimer is translated to the center via the relations

$$\begin{aligned} x_i &= x_i - CMx \\ y_i &= y_i - CMy \\ z_i &= z_i - CMz \end{aligned} \tag{3}$$

Afterward the center of mass of each monomer (CM1) was determined and the coordinates again translated to fulfill the constraint.

$$\begin{aligned} x_i &= x_i - CM1x \\ y_i &= y_i - CM1y \\ z_i &= z_i \end{aligned} \tag{4}$$

This method conserves energy completely so that microcanonical dynamics can be investigated.

The equilibrium properties reported in the following section were calculated with MD trajectories in both the canonical and microcanonical ensembles. The canonical trajectories were run, not necessarily to thermostat the system (the temperature as defined by the kinetic energy remained around 300 K, regardless), but to help ensure ergodicity. This can be a very real problem in biomolecular simulations because of the presence of numerous potential wells. Periodically randomizing the velocities effectively provides a new set of initial conditions to be averaged over and a new region of phase space to be explored.

The intramolecular potential used for the hydronium ion was obtained by *ab initio* calculations using the 6–31G* basis set at the restricted Hartree-Fock level. The resulting potential curves for the bond stretch and angle bend were fit with a Morse potential that was subsequently expanded about the minimum to obtain the harmonic force constants. The resulting parameters for the bond and angle force constants, and the equilibrium bond and angle distances were, respectively, k_b = 400 kcal/mol Å^{-2}, k_θ = 50 kcal/mol rad^{-2}, r_{eq} = 0.9517 Å, and θ_{eq} = 110.4°. The charges on the hydronium, $q_O = -0.755e$ and $q_H = 0.585e$, were obtained by a Mulliken population analysis, also using the above basis set. The Lennard-Jones parameters for the ion were taken to be the same as for TIP3P water.

In the calculation of the dipole-dipole correlation functions reported below, special care was taken to specify the coordinate system for which the dipole was determined. For a neutral molecule the dipole is independent of the coordinate system, but for a charged species this is not the case. This is a result of the expansion used in obtaining the expression for the multipoles. In displacing the entity some distance *dr*, one introduces an error to the expansion *Qdr*, where *Q* is the overall charge of the molecule. The obvious symmetry of the hydronium ion lends it to the calculation of the dipole about its center of charge. The center of charge (CC) is defined as

$$CC = \frac{\sum_{i=1}^{N} |q_i| r_i}{\sum_{i=1}^{N} |q_i|} \tag{5}$$

RESULTS

Table 1 lists the average coordinates of the hydronium oxygen for several representative trajectories. This work concentrated on the hydronium in the region of the dimer junction and within one of the monomers. The choice of monomer is strictly arbitrary because the dimer is symmetric. As can be seen from Table 1, the position of the hydronium is essentially the same between the b1 and b2 simulations. The hydronium settled at approximately the same location, therefore it was assumed that the information from the trajectories could be averaged and that nonergodicity was not a significant problem.

In the b1 simulations all channel waters remained within the confines of the channel. However, in the b2 simulations the end channel waters tended to diffuse from the mouth. These waters were replaced by bulk waters that were placed and equilibrated around the mouths of the channel. After equilibration the electrostatic and LJ interactions appeared to keep them in place.

Average water CM-CM distance

Figs. 1-3 show the average CM-CM distances among the channel water molecules. In the absence of the hydronium ion, the average distance between the centers of mass of adjacent waters was on the order of 2.8 Å (Fig. 1), which is in agreement with other simulations (Jordan, 1990; Chiu et al., 1989). This was also the case when the hydronium was buried within a monomer (Fig. 3). However, when the hydronium was located in the dimer junction, the average O-O distance varied somewhat between simulations b1 and b2 (Fig. 2). For b1, where the waters were originally placed

TABLE 1 Average coordinates, bond distances, and angles for the hydronium ion in Gramicidin A

No.	Initial condition	Length (ps)	⟨x⟩ (Å)	⟨y⟩ (Å)	⟨z⟩ (Å)	R_{OH} (Å)	HOH (deg)
1	b1	100	.805	−.194	.450	.9862	107.6
2	b1	50	−.612	−.324	.428	.9886	105.2
3	b2	69	.001	−.129	.358	.9908	108.6
4	b2	50	.021	−.247	.354	.9888	108.3
5	b2	50	−.126	−.202	.082	.9899	108.4
6	b1	100	−.362	−8.60	−1.06	.9988	106.2
7	b1	100	−.271	−8.67	−1.12	.9945	107.1
8	b2	60	−.314	−8.40	−.814	.9976	106.8
9	b2	50	.272	−8.32	−.423	.9960	106.7

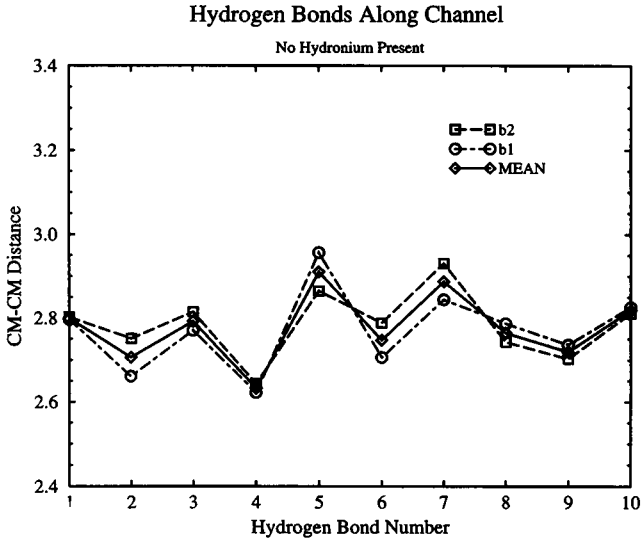

FIGURE 1 Average distance between the centers of mass of neighboring waters within gA in the absence of the hydronium ion for simulations b1 (*circle*), b2 (*square*), and their mean (*diamond*).

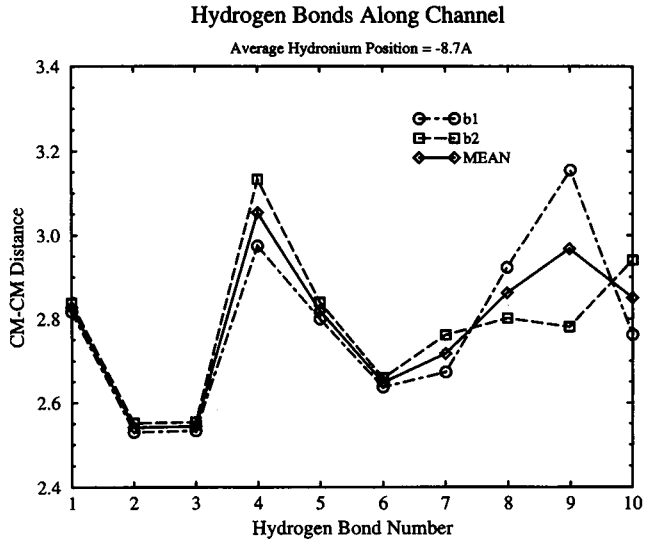

FIGURE 3 Average distance between the centers of mass of neighboring waters within gA with the hydronium ion within a monomer for simulations b1 (*circle*), b2 (*square*), and their mean (*diamond*).

2.25 Å apart, the average O-O distance was found to be ~2.66 Å, whereas for b2 (2.67 Å) it was 2.86 Å. Despite the differences between b1 and b2, in each case the average NN O-O distance of ~2.55 Å with the hydronium ion is considerably lower than the mean, whereas the O-O distance between the NN and NNN waters is consistently greater than the mean. This indicates a "break" in the hydrogen-bonded network following the formation of the hydronium-water cluster. The value of ~2.55 Å (averaging over b1 and b2) for the O-O distance with the NN water molecules is in good qualitative agreement with simulations of H_3O^+ in bulk water (Tuckerman et al., 1995; Lobaugh and Voth, 1996).

The break in the network may be the cause of the lower proton mobility in gA versus that in bulk water (1×10^{-3} cm^2/Vs (Akeson and Deamer, 1991) vs. 3.62×10^{-3} cm^2/Vs). Within gA there are minima about which the water molecules oscillate because of, at least in part, preferred binding sites within the channel. In this way, the water structure in gA resembles ice; in fact, it has been suggested that the mechanism by which protons diffuse through gA is similar to that by which they diffuse through ice (Levitt, 1984; Hladky and Haydon, 1972). Yet, the mobility of protons in gA may be somewhat lower than in ice, quite possibly as a result of a

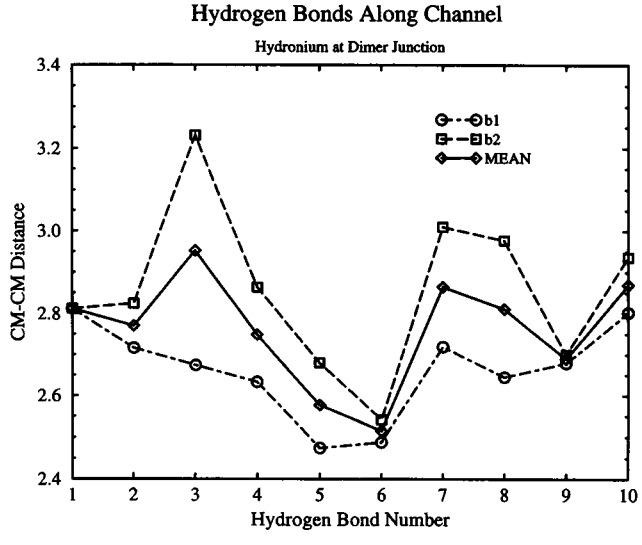

FIGURE 2 Average distance between the centers of mass of neighboring waters within gA with the hydronium ion at the dimer junction for simulations b1 (*circle*), b2 (*square*), and their mean (*diamond*).

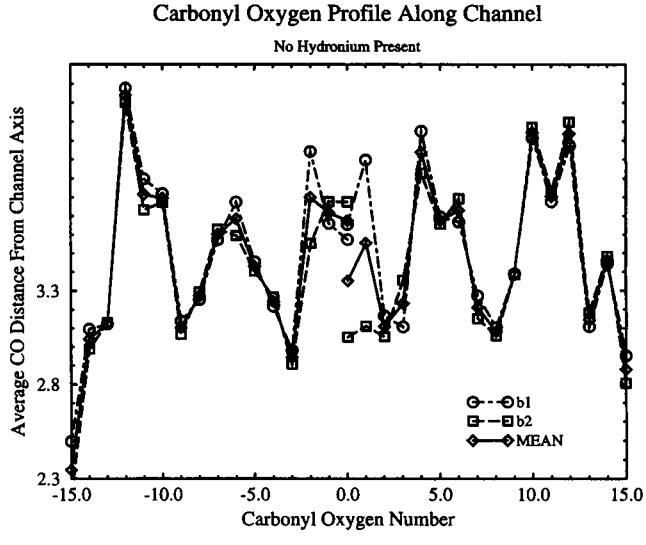

FIGURE 4 Average radial distance of carbonyl oxygens from the channel axis in the absence of hydronium ion for simulations b1 (*circle*), b2 (*square*), and their mean (*diamond*).

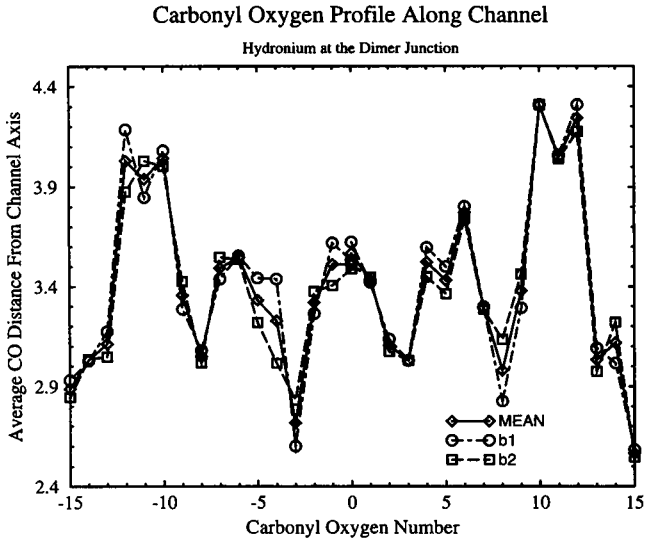

FIGURE 5 Average radial distance of carbonyl oxygens from the channel axis with the hydronium ion at the dimer junction for simulations b1 (*circle*), b2 (*square*), and their mean (*diamond*).

poorer hydrogen-bonded network within gA (Akeson and Deamer, 1991). Our results support this notion.

Carbonyl oxygen distance from the channel axis

In Figs. 4–6, the average carbonyl oxygen distance from the channel axis as defined earlier is shown. What is most striking is the rather pronounced drop in the O(C) distance in the vicinity of the hydronium when compared to the "pure water" channel (Fig. 4). When the hydronium is at the dimer junction (Fig. 5), one sees a preferred association with L-ALA3B in which the O(C) distance from the channel

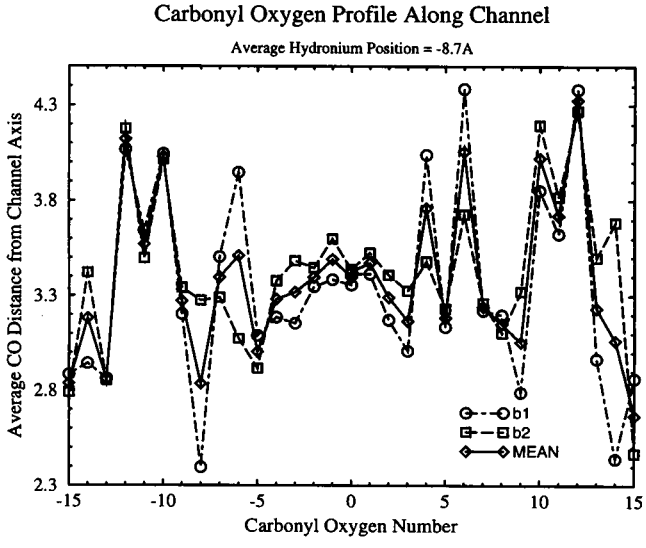

FIGURE 6 Average radial distance of carbonyl oxygens from the channel axis with the hydronium ion within a monomer for simulations b1 (*circle*), b2 (*square*), and their mean (*diamond*).

TABLE 2 The average hydrogen bond distances (*R*) and angles for the hydronium ion (within monomer) with neighboring carbonyl oxygens

Residue		b1	b2
D-VAL6B	*R* (Å)	2.92	1.79
	$H_2OHO(C)$ (deg)	89.27	158.91
D-ALA8B	*R* (Å)	2.52	4.13
	$H_2OHO(C)$ (deg)	121.89	37.23
L-TRP13B	*R* (Å)	2.168	2.54
	$H_2OHO(C)$ (deg)	122.70	103.36

axis drops ~0.3 Å to solvate the hydronium. When the hydronium is buried within a monomer, there is also a distortion of the backbone as D-Val8B is pulled down markedly from the 3.25-Å position of its pure water counterpart in the b1 simulation. In fact, the hydronium is preferentially hydrogen bound to D-Val8B and L-Trp13B. In previous studies of Na^+ in gA, the D-Val8 and L-Trp13 also participated in the ion's solvation along with D-Leu10 and L-Trp15 (Roux and Karplus, 1991). In the b2 simulation, whereas there is hydrogen bonding to D-Val18B and L-Trp13B, there is also considerable association with the D-Val6B carbonyl. Table 2 lists the average O-H-O angles of these carbonyl oxygens with the hydronium ion. It must be noted that what is apparently a rather poor hydrogen-bonded angle is an average value. That average also takes into account the instances in which the hydronium is not explicitly hydrogen bound to that carbonyl. The hydronium has, at its disposal, several carbonyls with which to bind in the channel.

The added interaction of the hydronium ion with the carbonyl oxygens could facilitate the proton transfer rate, or it could actually serve to inhibit proton migration. The CO-water hydrogen bond is known to be a rather strong one, being ~1.5 kcal/mol stronger than the water-water hydro-

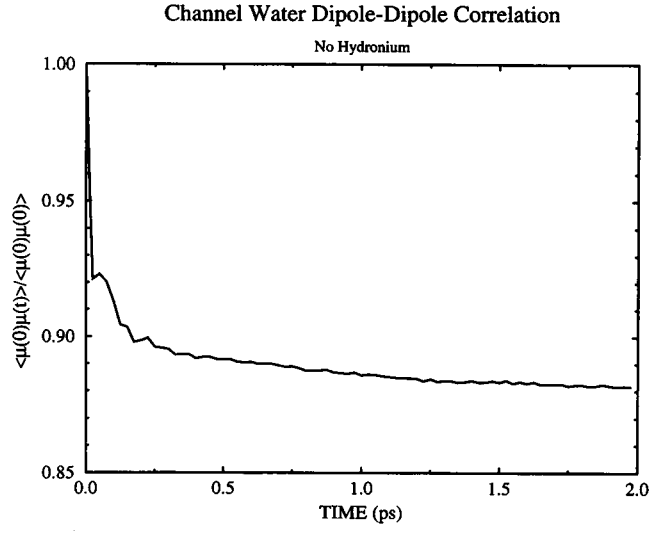

FIGURE 7 Dipole-dipole correlation function averaged over all channel waters in the absence of the hydronium ion.

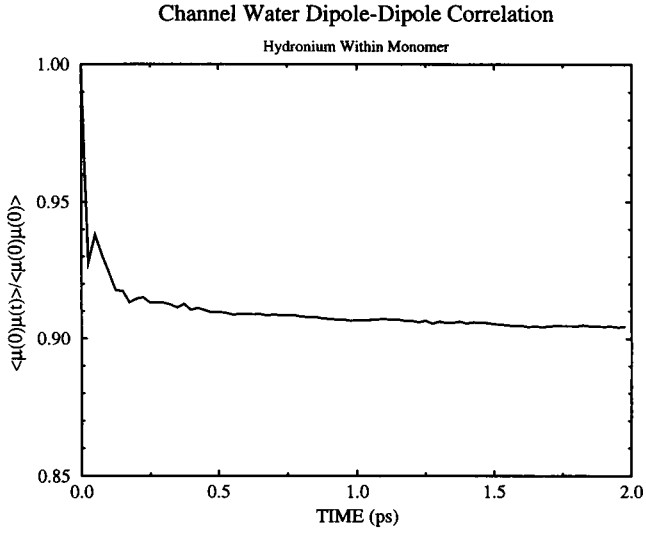

FIGURE 8 Dipole-dipole correlation function averaged over all channel waters with the hydronium ion within a monomer.

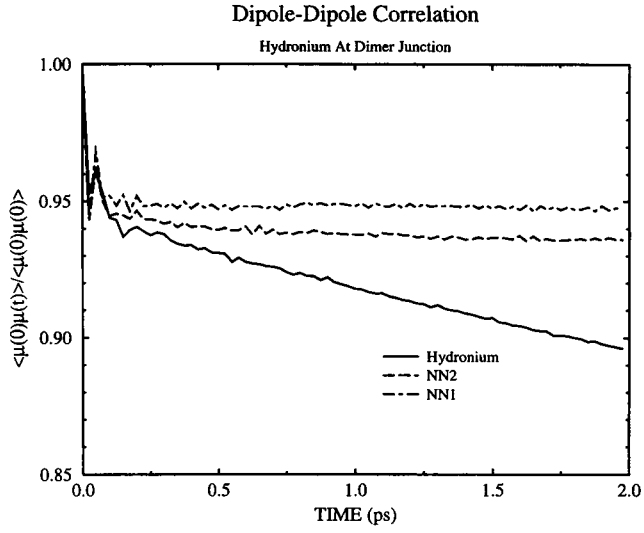

FIGURE 10 The dipole-dipole correlation function with the hydronium ion at the dimer junction for the hydronium ion (*solid line*), NN1 water (*long-short dashed line*), and NN2 water (*long-long dashed line*).

gen bond, which could keep the H_3O^+, as well as the channel waters, in place. The NN waters of the hydronium ion thus appear to be forced to withdraw from their nearest neighbors, creating the break in the hydrogen-bonded network as noted above, to effectively solvate the hydronium. Two recent studies of proton transfer in bulk water suggest that it is the fluctuation of the second solvation shell that is the rate limiting step in proton transfer (Tuckerman et. al. 1995; Lobaugh and Voth, 1996). Stated differently, what is needed for the transfer of the proton is the inward movement of an NNN acceptor from the second solvation shell while the NNN donor retreats. In light of the rather large NN-NNN water distance, it would seem that the carbonyl groups may actually serve to inhibit proton transfer. On the other hand, in gA these groups also help to solvate the charge associated with the excess proton. Assuming that one purpose of the second solvation shell is to solvate the newly formed hydronium ion during the proton transfer process, then the CO groups may be as important as the NNN water molecules in that regard. In other words, whereas the carbonyls appear to solvate and stabilize the break in the hydrogen-bonded network, they also participate in the key electrostatic interactions required for proton hopping in the channel. Again the "molecularity" of the channel is interestingly complex and not adequately described by a simple continuum picture.

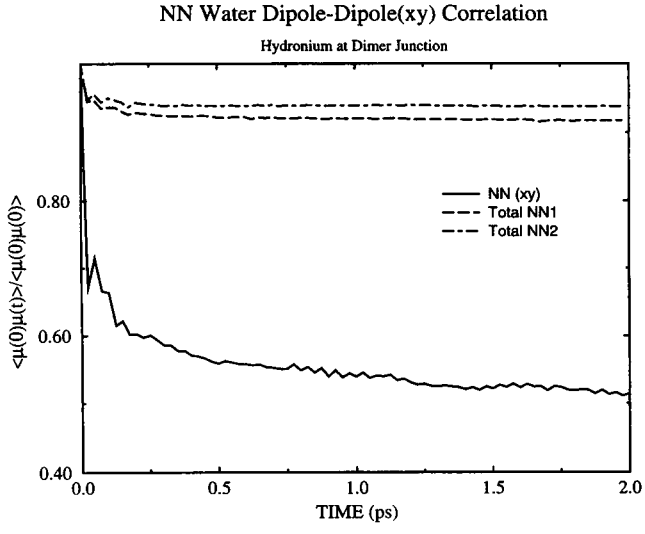

FIGURE 9 The dipole-dipole correlation function of the radial components of the dipole for the channel waters with the hydronium ion at the dimer junction.

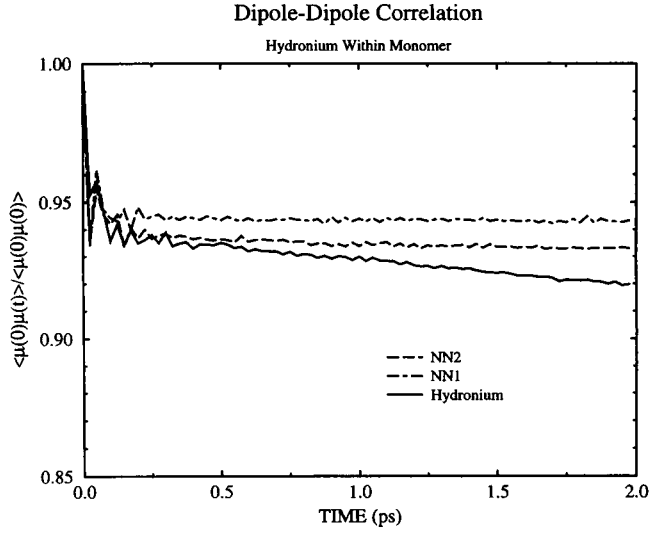

FIGURE 11 The dipole-dipole correlation function with the hydronium ion within a monomer for the hydronium ion (*solid line*), NN1 water (*long-short dashed line*), and NN2 water (*long-long dashed line*).

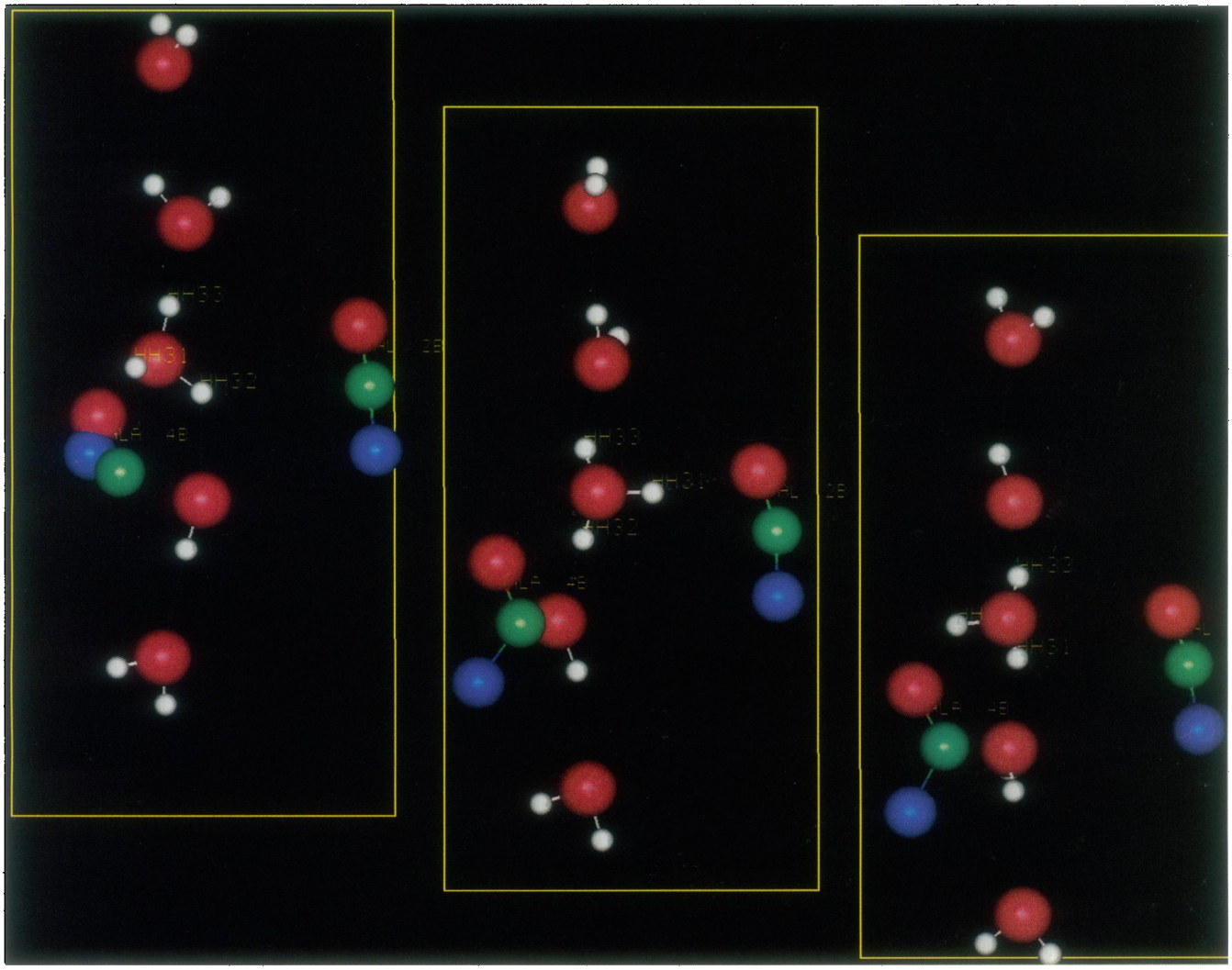

FIGURE 12 Three snapshots taken during the flipping of the hydronium ion at the dimer junction. A complete description of the events (including those pictured) are given in the text.

Reorientational dynamics

The reorientational dynamics of the hydronium ion and channel water molecules is also expected to play a key role in the proton migration mechanism through gA. As a result, the reorientational dynamics of the channel waters and hydronium were examined. The computed dipole-dipole correlation functions are depicted in Figs. 7–10. Within the time scale of the MD simulations, the channel water dipoles experience very little relaxation compared to that of bulk water. This is even more evident when a hydronium ion is present in the channel (Fig. 8). It would be incorrect, however, to suggest that this result indicates the waters are effectively locked in place. For there to be significant decay of the dipole-dipole correlation function the molecule must actually flip. Within the confines of such a narrow ion channel, this is not easy to do. However, significant rotation still exists in the region defined by the *xy* plane. Fig. 9 shows, for example, the dipole-dipole correlation function for the *x* and *y* components of the NN channel waters with the H_3O^+ ion at the dimer junction. Also shown is the total dipole correlation function for comparison. In the former case a more significant decay is observed. Although the channel waters do not flip, they are indeed spinning around about an axis defined by the hydrogen bond. The hydrogen bonds with the hydronium ion appear to remain intact, which is an important first requirement for proton hopping.

Another interesting feature is the relative decay of the hydronium dipole compared to that of its NN water molecules (Figs. 10–11). In particular, the decay of H_3O^+ when at the dimer junction is a result of the hydronium hydrogen bonding to more than one carbonyl, resulting in a wagging motion of sorts. In both the monomer and the dimer junction a complete flip of the dipole was recorded. This is a rare event occurring on the order of 100–200 ps (cf. Fig. 12). Interestingly, the hydronium actually follows a discrete path as it flips. Fig. 13, *a-f* shows the H_2O-H-O angles during a flip in the dimer junction. In these plots, H1 is the proton hydrogen bound to the carbonyl, whereas H2 and H3 are

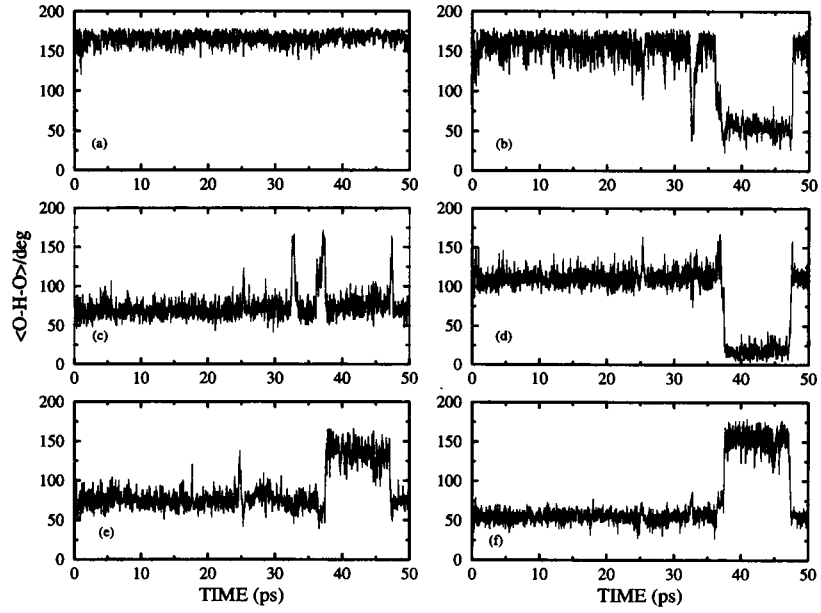

FIGURE 13 Hydrogen-bonded angle trajectories formed by the hydronium oxygen, its proton and the oxygen of its nearest neighbor, be it water or a carbonyl oxygen, for hydronium at the gA dimer junction: *a*) Proton 3 and its nearest neighbor channel water; *b*) Proton 1 and Ala3B; *c*) Proton 1 and Val1B; *d*)Proton 1 and ALA4; *e*) Proton 1 and the nearest neighbor water of proton 3; *f*)Proton 2 and Ala4B.

bound to an NN water. It is seen that the O-H3-O angle remains tightly around 170°C (Fig. 13 *a*). It is about this axis that the hydronium rotates. At ~32 ps, a thermal fluctuation causes H1 to flip from ALA3B to VAL1B (Fig. 13, *b-c*) and then return. At ~36 ps, H1 goes to ALA3 then to VAL1B (Fig. 13, *c-d*) and from there to the NN of H2 (Fig. 13 *e*). H2 jumps to ALA3B as H1 moves from VAL1B to the NN water (Fig. 13 *f*). These jumps are discrete in that no smooth rotation was observed. Apparently the hydronium sampled the several different local minima present at the junction. The hydronium within the monomer also experienced a flip, but this was more of an umbrella mode inversion. In other words, only one hydrogen bond was broken during the event. The hydrogen bonds with the NN waters remained intact whereas the remaining proton flipped from VAL6B to Val8B. This can be seen in Fig. 14.

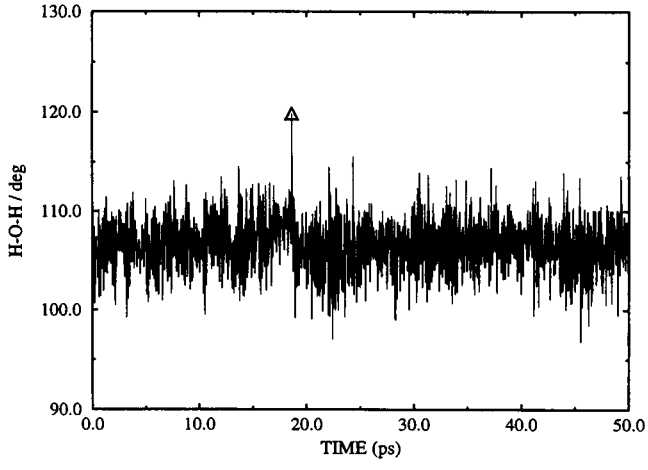

FIGURE 14 The average H-O-H angle for the hydronium ion within a monomer as a function of time.

Here, it is seen that the HOH angles of the hydronium at time ~18.5 ps were 120°C, indicating the planar structure necessary for inversion.

CONCLUSIONS

This study has been concerned with the structural and dynamical properties of hydronium in the ion channel gramicidin A. The focus has been on those effects that are likely to influence proton transport through the channel. The hydronium-water NN distance was found to be comparable to that in simulations of proton transfer in bulk water, but there are significant breaks in the NN-NNN water hydrogen-bonded distances. This result argues against a collective transport mechanism for the proton through the channel. On the other hand, it is also clear that the carbonyl groups play an important role in hydronium ion solvation and, therefore, are also likely to play an important role in the proton transfer process. As the carbonyls are believed to solvate the waters well enough to stabilize the break in the hydrogen-bonded network, they may also sufficiently solvate the hydronium to aid in the hop of the proton.

Regarding the dynamics of the hydronium, there is a certain degree of rotational freedom, especially at the dimer junction. In that case, the axis about which the rotation occurs is that of the hydrogen bond with an NN water. If the rotation were to occur through the dipole axis little decay would be noted and some interaction would be required to act as the pivot point. The dipole of the hydronium is approximately orthogonal to the channel axis. A strong long lasting hydrogen bond with the proton of a neighboring amine would be necessary for the rotation; however, such an association was not observed. The rotation of the hydronium at the channel junction involves a series of discrete jumps that can be viewed as the ion following a path of local

potential minima that are visited during the thermal fluctuations of the system. This flipping is a rare event, happening on a time scale of 100–200 ps. The water dipoles remained aligned in the present simulations, whereas others have observed a complete reorientation at ~200 ps in the absence of a hydronium ion within the channel. This time scale is longer than any one of our trajectories, but such a flipping would be rather energetically costly with the hydronium in the channel because the dipoles would then be mal-aligned. It can therefore be concluded that the hydronium ion causes some additional degree of water ordering in the channel.

This research was supported by a Fellowship in Science and Engineering from the David and Lucile Packard Foundation to G. A. Voth.

REFERENCES

Akeson, M., and D. W. Deamer. 1991. Proton conductance by the gramicidin water wire. Model for proton conductance in the F_1F_0 ATPases? *Biophys. J.* 60:101–109.

Anderson, H. C. 1980. Molecular dynamics simulations at constant pressure and/or temperature. *J. Chem. Phys.* 72:2384–2393.

Andersen, O. S. 1984. Gramicidin channels. *Ann. Rev. Physiol.* 46: 531–548.

Arseniev, A. S., V. F. Bystrov, T. V. Ivanov, and Y. A. Ovchinnikov. 1985. 1H NMR study of gramicidin-A transmembrane ion channel. Head-to-Head right-handed, single stranded helices. *FEBS Lett.* 186:168–174.

Cao, Y., G. Varo, M. Chang, B. Ni, R. Needleman, and J. K. Lanyi. 1991. Water is required for proton transport from aspartate-96 to the bacteriorhodopsin Schiff base. *Biochemistry.* 30:10972–10979

Chiu, S. W., S. Subramaniam, E. Jakobsson, and J. A. McCammon. 1989. Water and polypeptide conformations in the gramicidin channel. *Biophys. J.* 56:253–261.

Deamer, D. W., and J. W. Nichols. 1983. Proton-hydroxide permeability of liposomes. *Proc. Natl. Acad. Sci.* USA 80:165–168.

Deamer, D. W. 1987. Proton permeation of lipid bilayers. *J. Bioenerg. Biomembr.* 19:457–479.

Deisenhofer, J., and H. Michel. 1989. Nobel lecture. The photosynthetic reaction centre from the purple bacterium *Rhodopseudomonas viridis*. *EMBO. J.* 8:2149–2170.

Finkelstein, A., and O. S. Andersen. 1981. The Gramicidin A channel: a review of its permeability characteristics with special reference to the single-file aspect of transport. *J. Memb. Biol.* 59:155–171.

Henderson, R., J. M. Baldwin, T. A. Ceska, F. Zemlin, E. Beckmann, and K. H. Downing. 1990. Model for the structure for bacteriorhodopsin based on high resolution cryo-microscopy. *J. Mol. Biol.* 213:899–929.

Jordan, P. C. 1990. Ion-water and ion-peptide correlations in a gramicidin-like channel. A molecular dynamics study. *Biophys. J.* 58:1133–1155.

Levitt, D. G., S. R. Elias, and J. M. Hautman, 1978. Number of water molecules coupled to the transport of sodium, potassium, and hydrogen ions via gramicidin, nonactin, or valinomycin. *Biochim. Biophys. Acta.* 512:436–451.

Lobaugh, J., and G. A. Voth. 1996. The quantum dynamics of an excess proton in water. *J. Chem. Phys.* 104:2056–2069.

Myers, V. B., and D. A. Haydon. 1972. Ion transfer across lipid membranes in the presence of gramicidin A. II. The ion selectivity. *Biochim. Biophys. Acta.* 274:313–322.

Nagle, J. F., and S. Tristram-Nagle, 1983. Hydrogen bonded chain mechanisms for proton conduction and proton pumping. *J. Membr. Biol.* 74:1–14.

Nichols, J. W., and D. W. Deamer, 1978. Net proton-hydroxyl permeability of large unilamellar lipsomes measured by an acid-base titration technique. *Proc. Natl. Acad. Sci. USA.* 77:2038–2042.

Nichols, J. W., and D. W. Deamer. 1980. *In:* Frontiers of Bioenergetics. P. L. Dutton, J. S. Leigh, and A. Scarpa, editors. Academic, New York. 1273–1283.

Nichols, J. W., A. D. Bangham, M. Hill, and D. W. Deamer, 1980. Measurement of net proton-hydroxyl permeability of large unilamellar liposomes with the fluorescent pH probe 9-Aminoacridine. *Biochim. Biophys. Acta.* 596:393–403.

Nicholson, L. K., and T. A. Cross. 1989. The gramicidin cation channel: an experimental determination of the right handed helix sense, and verification of β-type hydrogen bonding. *Biochemistry.* 28:9379–9385.

Papadopoulos, G., N. A. Dencher, G. Zaccai, and G. Buldt. 1990. Water molecules and exchangeable hydrogen ions at the active centre of bacteriorhodopsin localized by neutron diffraction. Elements of the proton pathway? *J. Mol. Biol.* 214:15–19.

Roux, B., and M. Karplus. 1994. Molecular dynamics simulations of the gramicidin channel. *Annu. Rev. Biophys. Biomol. Struc.* 23:731–761.

Roux, B., and M. Karplus. 1993. Ion transport in the gramicidin channel: free energy of the solvated right-handed dimer in a model membrane. *J. Am. Chem. Soc.* 115:3250–3260.

Roux, B., and M. Karplus. 1991. Ion transport in a gramicidin-like channel: structure and thermodynamics. *Biophys. J.* 59:961–981.

Sarges, R., and B. Witkop. 1965. Gramicidin A. V. The structure of valine- and isoleucine gramicidin A. *J. Am. Chem. Soc.* 87:2011–2020.

Tuckerman, M., K. Laasonen, M. Sprik, and M. Parrinello. 1995. *Ab initio* molecular dynamics simulation and transport of hydronium and hydroxyl ions in water. *J. Chem. Phys.* 103:150–161.

Urry, D. W. 1971. The gramicidin A transmembrane channel: a proposed πLD helix. *Proc. Natl. Acad. Sci. USA.* 68:672–676.

Wooley, G. A., and B. A. Wallace. 1992. Model ion channels: gramicidin and alamethicin. *J. Membr. Biol.* 129:109–136.